



# Polyoxazolines based lipid nanocapsules for topical delivery of antioxidants

L. Simon<sup>a</sup>, V. Lapinte<sup>a</sup>, L. Lionnard<sup>b</sup>, N. Marcotte<sup>a</sup>, M. Morille<sup>a</sup>, A. Aouacheria<sup>b</sup>, K. Kissa<sup>c</sup>, J.M. Devoisselle<sup>a</sup>, S. Bégu<sup>a,\*</sup>

<sup>a</sup> ICGM, Univ Montpellier, CNRS, ENSCM, Montpellier, France

<sup>b</sup> ISEM, Univ Montpellier, CNRS, EPHE, IRD, Montpellier, France

<sup>c</sup> DIMNP, Univ Montpellier, CNRS, Montpellier, France

## ARTICLE INFO

### Keywords:

Antioxidant  
Lipid nanocapsules  
PEG free  
Polyoxazolines  
Skin protection  
Topical delivery

## ABSTRACT

Nano-sized lipid formulations offer a great potential for topical delivery of active compounds to treat and prevent human skin damages. Of particular importance is the high loading of hydrophobic molecules, the long-term stability and the auspicious penetration capacity especially reached when using lipid nanocapsules (LNC). Unfortunately, their formation currently relies on a phase inversion process that only operates when using a poly (ethylene glycol) (PEG) based surfactant belonging to the controversial PEG family that was subject of clinical awareness. The present study proposes an alternative to this overused polymer in formulations by designing LNC made of harmless amphiphilic polyoxazolines (POx). Implementing a short sonication step in the process allowed well-defined spherical nanoparticles of ~30 nm to be obtained. The structure of the so called LNC POx was composed of an oily core surrounded by a rigid shell of phospholipids and POx, which ensures a high stability over time, temperature, centrifugation and freezing. Encapsulation of the natural quercetin antioxidant led to a drug loading three times higher than for LNC constituted of PEG (LNC PEG). The antioxidant activity of loaded LNC POx was tested on mice fibroblasts and human keratinocytes after exposure to free radicals from peroxides and UVB irradiation, respectively. The radical scavenging capacity of quercetin loaded in the LNC POx was preserved and even slightly enhanced compared to LNC PEG, highlighting the POx value in nanoformulations.

## 1. Introduction

Environmental factors such as UV radiations, pollution or tobacco have a negative impact on human skin by accelerating skin aging and potentially leading to skin cancer (Krutmann et al., 2017). Human skin acts as a barrier against this hostile environment thanks to its unique structure and composition. The main protective layer, *stratum corneum* (SC), ensures stiffness and permeability to the skin due to corneocyte cells embedded in a lipid matrix (Elias, 1983). The vital barrier function of the SC then becomes a hurdle to overcome when delivery of active compound (AC) to the deepest layer of the skin is concerned (e.g. the imiquimod with antimitotics properties). Indeed, only small (< 500 Da) uncharged lipophilic (logP 1–3) molecules are able to go through the SC (Roberts et al., 2017), whereas the largest or charged ones need to be formulated for a successful delivery through the skin. Topical formulations of lipid nano-sized vectors are one of the preferred solutions since their size allows for enhanced penetration (Hatahet et al., 2016). As a matter of fact, solid or polymeric nanoparticles and colloidal lipid nanocarriers loaded with AC were shown to induce

therapeutic effect, crossing through the SC to reach their site of action (Roberts et al., 2017). Formulating the nanovector with lipid-based colloids increases the epidermis penetration thanks to a fluidization mechanism of the SC lipid barrier. Among the colloidal formulations developed, solid lipid nanoparticle (SLN), nanostructured lipid carrier (NLC), liposome and lipid nanocapsule (LNC) are increasingly exploited due to their enhanced efficiency (Roberts et al., 2017). It has to be mentioned that adding chemical penetration enhancers (CPE) to the topical formulations facilitates the passive diffusion of the AC once into the deepest layer of the skin (Dragicevic et al., 2015).

The structure of the main lipid-based formulations used for topical delivery of AC is schematically depicted in Table 1. Also listed are the composition of the lipid formulations, some physical parameters and the advantages and drawbacks of the corresponding nanovector. Liposomes, the oldest known lipid-based formulation systems, consist of a lipid bilayer of phospholipids delimiting an inner aqueous core. Such structure allows liposomes to encapsulate either hydrophilic or hydrophobic active pharmaceutical ingredients that can diffuse through the skin layers, after the liposomes have adsorbed on the skin surface and

Abbreviations: HPH, high pressure homogenizer; PIT, phase inversion process; DL, drug loading

\* Corresponding author.

E-mail address: [sylvie.begu@enscm.fr](mailto:sylvie.begu@enscm.fr) (S. Bégu).


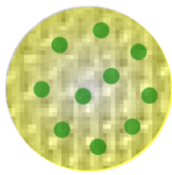
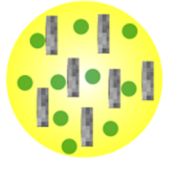
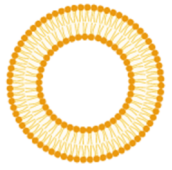

<https://doi.org/10.1016/j.ijpharm.2020.119126>

Received 18 October 2019; Received in revised form 4 February 2020; Accepted 5 February 2020

Available online 16 February 2020

0378-5173/© 2020 Elsevier B.V. All rights reserved.

**Table 1**  
Properties and features of NLC, SLN, LNC and liposome formulations.

Type of lipid formulation	Solid lipid nanoparticles (SLN)	Nanostructured lipid carriers (NLC)	Liposomes	Lipid nanocapsules (LNC)
				
Composition	Solid lipid core with polymer shell (Schäfer-Korting et al., 2007)	Mixture of solid and liquid lipid core and surfactant layer (Schäfer-Korting et al., 2007)	Lipid bilayer enclosing an aqueous core (Zhai and Zhai, 2014)	Liquid lipid core surrounded by a solid membrane from lecithin and surfactant (Huynh et al., 2009)
Size	40–1000 nm (Sala et al., 2018)	40–1000 nm (Sala et al., 2018)	20–3000 nm (Sala et al., 2018)	20–100 nm (Huynh et al., 2009)
Preparation method	Hot or cold HPH (Schäfer-Korting et al., 2007) or microemulsion technique (Montenegro et al., 2016)	Hot or cold HPH (Schäfer-Korting et al., 2007) or microemulsion technique (Montenegro et al., 2016)	– Bangham method – Detergent depletion method – Injection method... (Maherani et al., 2011)	PIT (Heurtault et al., 2002)
Advantages	Biocompatibility, drug protection against degradation (Sala et al., 2018); low toxicity and feasible scaling up (Zhai and Zhai, 2014)	Higher stability and DL than SLN (Montenegro et al., 2016)	Flexibility and deformability; high DL of hydrophilic AC (Sala et al., 2018)	Better encapsulation and greater stability (Huynh et al., 2009) than SLN and NLC; excellent tolerability for dermal application (Zhai and Zhai, 2014)
Disadvantages	High degree of order leading to low DL (Zhai and Zhai, 2014)	Lower skin permeation than LNC (Zhai and Zhai, 2014)	Low capacity to encapsulate lipophilic drug; presence of traces of organic solvent, unstable in biological fluid (Huynh et al., 2009)	Low DL of hydrophilic AC (Huynh et al., 2009)

merged with the lipid matrix (Sala et al., 2018). Contrary to liposomes, SLN, NLC and LNC possess an oily core. SLN are composed of a solid lipid core at room temperature that is stabilized by a polymer shell, whereas the NLC core is made of a mixture of liquid and solid lipids surrounded by a surfactant layer (Schäfer-Korting et al., 2007). SLN and NLC interact with the SC and create a lipid rearrangement facilitating drug penetration (Garcés et al., 2018). Only LNC possesses an oily liquid core surrounded by a rigid surfactant and phospholipid membrane (Huynh et al., 2009).

Among all those lipid based nanoformulations, LNC demonstrates higher performances for topical delivery of a model compound as AC. Indeed, they allow similar permeation as SLN and NLC with a reduced intradermal drug accumulation and exhibit a better stability and a higher loading efficiency (Abdel-Mottaleb et al., 2011). LNC are usually formed by a low energy process using the phase inversion method, which was initially developed by Heurtault et al. (Heurtault et al., 2002). It relies on the properties of the nonionic surfactant polyethylene glycol (15)-hydroxystearate, which possesses a temperature-dependent hydrophilic-lipophilic balance (HLB) allowing emulsions to switch from oil in water to water in oil (Anton et al., 2007). After three heating and cooling cycles, the induced phase inversion is cooled down and diluted leading to LNC with a size of 20–100 nm (Huynh et al., 2009). The *in vitro* and *in vivo* skin penetration study of the LNC prepared with ropivacaine as an AC showed an apparent morphology change of the SC, proving the transdermal delivery potency of this type of formulations (Zhai et al., 2014). Moreover, studies for the topical delivery of quercetin showed superior penetration capacity of LNC compared to liposomes and smart crystals formulations, and the possibility to deliver the antioxidant to the viable epidermis upon application to human skin *in vivo* (Hatahet et al., 2018). This makes LNC the most promising lipid formulation for skin penetration and delivery to the epidermis.

Despite all the advantages of LNC for topical delivery, this lipid-based formulation suffers from its exclusive reliance on polyethylene glycol (PEG) surfactant. Indeed, PEG was proved to generate an immune response (Zhang et al., 2016; Lubich et al., 2016) and accumulate in body tissues (Rudmann et al., 2013; Viegas et al., 2018). This represents a major drawback in the development of LNC for many applications ranging from nanomedicine to cosmetics. The clinical awareness on PEG overuse makes it particularly important to design new biocompatible surfactants as an alternative to the controversial PEG. In that context, we aimed at developing LNC devoid of PEG.

We proposed to use poly(2-R-2-oxazoline) (POx), a class of polymers with a peptidomimetic structure belonging to the polyamide family, as a surfactant for LNC formation. Indeed POx offers interesting properties such as its cytocompatibility and hemocompatibility (Lorson et al., 2018), in addition, it possesses a stealth behavior (Zalipsky et al., 1996) and its HLB is easily tunable through synthesis (Guillerm et al., 2012). It also holds great promise as a platform polymer for drug delivery (Moreadith et al., 2017). As recently reviewed by Luxenhofer (Lorson et al., 2018), POx-based formulations with solid dispersions (Paclitaxel, curcumin, Doxorubicin) and drug formulations have already been described as well as theranostic drug delivery systems incorporating proteins and gene complexes and using partially hydrolyzed POx (Dargaville et al., 2018). Recently, we also demonstrated the ability of POx to formulate stable mixed-micelles loaded with quercetin while maintaining its antioxidant activity (Simon et al., 2019).

In the present work, we evaluated the potency of POx to stabilize lipid nanocapsules, called LNC POx, for topical delivery. A new process allowing stable LNC POx to be obtained was developed. LNC POx was loaded with a natural flavonoid antioxidant, the quercetin (Q), which was previously studied for topical delivery in various formulations (Nagula and Wairkar, 2019). The model compound was chosen due to its readily assessable, reported antioxidant activities (Hatahet et al., 2016) and used to prove LNC POx efficacy as a topical platform to protect and maintain bioactivity. The physico-chemical and mechanical

properties of LNC POx were evaluated, and their effect on the cell viability of mice fibroblasts was assessed. The antioxidant activity of quercetin loaded in LNC POx was evaluated. Finally, a comparison study of the radical scavenging capacity of Q-LNC POx and Q-LNC PEG on mice fibroblasts and human keratinocytes was performed to evaluate the ability of Q-LNC POx to protect cells from an excess of radical species.

## 2. Materials and methods

### 2.1. Materials

Quercetin (95% HPLC), DPPH (2,2-diphenyl-1-picrylhydrazyl), phenazine methosulfate (PMS), *tert*-butyl hydroperoxide solution (TBHP) 70% in water, acetonitrile, diethyl ether, methanol, acetone, phosphoric acid and 2,7-dichlorofluorescein diacetate (DCFDA) were purchased from Sigma Aldrich (Germany). Tween 80® (polysorbate 80) was purchased from BASF (Germany) and 3-(4,5-dimethylthiazol-2-yl)-5-(3-carboxymethoxyphenyl)-2-(4-sulfophenyl)-2H-tetrazolium (MTS) was from Promega (USA). Lipophilic Labrafac® (caprylic acid triglycerides) was brought from Gattefossé (Saint-Priest, France) and Lipoid S75® (fatfree soybean phospholipids with 70% phosphatidylcholine) was kindly provided by Lipoid (Ludwigshafen, Germany). Sodium chloride (NaCl) was bought from VWR. MilliQ water was obtained from Milli-Q Gradient A10 (Merck Millipore, Germany) apparatus. Chloroform (for HPLC, stabilized with ethanol) was bought from Carlo Erba (Carlo Erba Reagent, Spain). All the reagents were used without further purification. Spectra/Por 6 dialysis membranes pre-wetted RC tubing with 0.5–1 kDa MWCO were purchased from Spectrum Labs (USA).

### 2.2. Methods

#### 2.2.1. LNC POx formulation

The lipid nanocapsule (LNC POx) were obtained by mixing Labrafac®, Lipoid® S75, Milli-Q water, NaCl and amphiphilic poly-oxazoline (POx, C<sub>16</sub>POx<sub>15</sub>). C<sub>16</sub>POx<sub>15</sub> was synthesized as described in (Simon et al., 2019). Three heating and cooling cycles (85–30 °C) of the mixture were performed under magnetic stirring. The solution was placed in an ice bath and sonicated for 4 min at 30% amplitude with a Digital Sonifier 250 sonication probe (Branson Ultrasonics Corporation, USA) using a Microtip 64-247A. Then quercetin was added as a powder to the solution and additional heating and cooling cycle was carried out. A last heating to 80 °C was then performed before addition of 2.5 mL of MilliQ water at 4 °C. The quercetin loaded LNC (Q-LNC POx) obtained was cooled down under magnetic stirring. The unloaded quercetin was separated by filtration through 0.2 µm syringe filter (Whatman). Blank-LNC (B-LNC POx) was prepared by the same method, except that quercetin was removed from the process.

The composition was optimized after doing a ternary phase diagram (POx, Labrafac® oil, water) for which the concentration of Lipoid® S75 and NaCl were fixed at 1.5% and 3% (w/w) respectively. The composition (w/w) containing 20% of POx, 15% Labrafac®, 65% water (w/w) and 3% of quercetin was selected for its stability and high drug loading (Section 2.2.6).

All the analyses described below were performed on freshly prepared LNC POx preparations. The LNC stabilized by PEG, called LNC PEG, were prepared according to the protocol for quercetin LNC 20 nm developed by Hatahet et al. (2017).

#### 2.2.2. Dynamic light scattering (DLS) and electrophoretic mobility measurement

Zetasizer NanoZS apparatus (Malvern Instruments, UK) equipped with a He-Ne laser (632.8 nm) was used to evaluate the hydrodynamic diameter and polydispersity index (PDI) of LNC POx (20 µL in 1980 µL of MilliQ water) at 20 °C at scattering angle of 173°. Zeta potential was

measured on 1000 µL of diluted LNC solutions in disposable capillary cell (Malvern Instruments, UK). All the results were average of three independent measurements.

#### 2.2.3. Stability of LNC

After preparation, the stability study was conducted at 4, 25 and 37 °C for the B-LNC POx and at 4 °C for the Q-LNC. The stability of the LNCs was assessed by measurements of the hydrodynamic diameter and PDI (see Section 2.2.2). Side studies of LNC stability were conducted using centrifugation at 15000 rpm for 15 min and freezing at –22 °C in a freezer. The hydrodynamic diameter and PDI were measured at described in Section 2.2.2.

The stability of Q-LNC POx at 25 °C was also evaluated by studying the *in vitro* release of quercetin diffusing through a nitrocellulose dialysis membrane (12–14 MWFC Spectra/Pore dialysis membrane from Spectrum laboratories, INC USA). The receptor medium was composed of 40 mL PBS at pH 7.4 with 2 wt% Tween® 80. The quercetin concentration released after 1, 2, 3, 4, 5, 6 and 7 h was measured by HPLC (Section 2.2.7).

#### 2.2.4. Transmission electron microscopy (TEM)

Transmission electron microscopy was performed on a TEM Jeol 1400 PLUS apparatus (Jeol. Ltbd, Tokyo, Japan) equipped with a Jeol 2K/2K camera. The samples were preliminarily diluted 1000 times before deposition on grids (type Cu formvar carbon) and were negatively colored with an aqueous uranyl acetate solution at 1.5 wt% and pH 5.

#### 2.2.5. Atomic force microscopy (AFM)

Atomic force microscopy was performed on Nanoman (Bruker Instrument) and monitored by Nanoscope V software. The LNC samples were diluted 100 times in MilliQ water and 5 µL of the solution was deposited on a silicon wafer. The tapping mode and harmonix mode were used after drying of the drop at 37 °C. For the tapping mode, PPP NCL tips (Nanosensors) were used at the resonance frequency of 157 kHz. Various amplitude setpoints were tested (from 500 to 250 mV) to modify the resulting force applied onto the sample. The harmonix mode was carried out using HMX-S tips (Bruker Instruments) by applying a force of 10–20 nN with a vertical resonance frequency of 48 kHz and horizontal of 791 kHz. No morphology modification of the LNC was observed.

#### 2.2.6. Encapsulation efficacy (EE) and drug loading capacity (DL)

Drug loading (DL) and encapsulation efficacy (EE) were respectively calculated using the following equations:

$$\text{Drug loading (\%)} = \frac{[\text{mass of quercetin}]}{[\text{total mass}]} \times 100 \quad (1)$$

where total mass represents the mass of POx, Labrafac and quercetin.

$$\text{Encapsulation efficacy (\%)} = \frac{[\text{amount of encapsulated quercetin}]}{[\text{amount of quercetin initially loaded}]} \times 100 \quad (2)$$

The quercetin loaded in Q-LNC POx was quantified by HPLC (Section 2.2.7) after filtration of the solution through a 0.2 µm filter (Whatman) to remove the residual unloaded quercetin.

#### 2.2.7. HPLC analysis

High Pressure Liquid Chromatography (HPLC) analysis of quercetin was performed on LC6-2012HT apparatus (Shimadzu, Kyoto, Japan) using a ProntoSIL C18 column (120-5-C18 H5.0 µm, 250 × 4.0 mm). The detection was achieved using a UV-vis detector (Shimadzu, Kyoto, Japan) at 368 nm (Yang et al., 2009). Acetonitrile/phosphoric acid at 0.2 wt% and pH = 1.9 (40/60%v) was used as mobile phase. The calibration curve was performed with solutions of quercetin in methanol from 1 to 100 µg/mL with a good linearity ( $r^2 = 0.9999$ ). The flow rate

was 1 mL min<sup>-1</sup>. To determine the concentration of quercetin released to the aqueous medium receptor (see stability study of LNC, [Section 2.2.3](#)) a calibration curve realized in PBS buffer at pH 7.4 and Tween® 80 (2 wt%) from 0.1 to 4 µg/mL ( $r^2 = 0.9996$ ) was used.

### 2.2.8. In vitro antioxidant activity

The antioxidant activity of Q-LNC POx was determined from the reactivity of quercetin towards the free radical 2,2-diphenyl-1-picrylhydrazyl (DPPH°) ([Blois, 1958](#)). It was calculated from the decrease of the DPPH° radical absorbance at 517 nm using the following equation (Eq. (3)):

$$\text{DPPH}^\circ \text{ scavenging (\%)} = \frac{\text{Absorbance of control} - \text{Absorbance of sample}}{\text{Absorbance of control}} \times 100 \quad (3)$$

where *Absorbance of control* corresponds to the absorbance of a 100 µM DPPH° solution. Note that the concentration of quercetin loaded in Q-LNC POx (2.5, 5, 7.5, 10, 12.5, 15 µM) was lower than that of DPPH°.

### 2.2.9. Cell culture

Mice fibroblasts cell lines (NIH3T3) were purchased from American Type Cell Culture organization (USA). Cells were maintained in Dulbecco's Modified Eagle Medium (DMEM) (Gibco) supplemented with 10% fetal bovine serum (Life Technologies), 1% L-glutamine and 1% penicillin/streptomycin equivalent to a final concentration of 2 nM for glutamine, 100 U mL<sup>-1</sup> for penicillin and 100 µg mL<sup>-1</sup> for streptomycin. They were incubated at 37 °C in humidified 5% CO<sub>2</sub> atmosphere.

Normal Human Epidermal Keratinocytes (NHEK) were purchased from Promocell (C-123003) and cultured at 37 °C in keratinocyte basal medium (C-20216 Promocell) supplemented with the supplement mix keratinocyte from Promocell (C-39016) under a humidified atmosphere containing 5% CO<sub>2</sub>. Cells were seeded to reach approximately 80% confluency at the time of treatment or irradiation. UVB irradiation was performed using a BS-02 UV irradiation chamber (Dr. Gröbel UV-Elektronik GmbH, Ettlingen, Germany). The lamp emits UVB irradiation with a peak at 311–312 nm and partially excludes shorter wavelengths, such as UVA.

### 2.2.10. Cell viability

NIH3T3 cells were seeded at 20,000 cells/cm<sup>2</sup> in 96 well plate and incubated for 24 h at 37 °C, 5% CO<sub>2</sub> to allow cell adhesion. Cells were treated or not (control) with quercetin, POx (B-LNC POx, Q-LNC POx) and PEG (B-LNC PEG, Q-LNC PEG) preparation. After 24 h of exposure, a CellTiter 96® Aqueous Non-Radioactive Cell Proliferation Assay (Promega, USA) was used to evaluate the cell viability following the manufacturer's instructions. The absorbance was recorded at 490 nm using Multiskan™ GO Microplate Spectrophotometer (Thermo Scientific™, Waltham, Massachusetts, USA). Absorbance of the basal media (with no cells and no treatment) was subtracted to the recorded absorbance for all conditions. Values of treated cells were normalized to non-treated cells (100% intensity).

### 2.2.11. Antioxidant effect of quercetin on TBHP treated NIH3T3 cells

NIH3T3 cells were seeded at 20,000 cells/cm<sup>2</sup> in a 96 well black plate with clear bottom (Corning® Massachusetts, USA) and incubated 24 h at 37 °C, 5% CO<sub>2</sub> to allow cell adhesion. Then B-LNC (POx and PEG), crude quercetin, or Q-LNC (POx and PEG) possessing an equivalent quercetin concentration of 5 µg/mL were added and incubated for another 24 h in supplemented DMEM. Cells were washed twice with PBS before addition of 200 µL of 2,7-dichlorofluorescein diacetate (DCFDA) reagent (20 µM in DMEM without phenol red). The serum free medium used provides reliable data by avoiding deacetylation of the DCFDA into non fluorescent compound that could later be oxidized by reactive oxygen species (ROS) into dichlorofluorescein

(DCF). After 30 min of incubation at 37 °C, 5% CO<sub>2</sub>, cells were rinsed with PBS and placed in 200 µL DMEM without phenol red. A solution of *tert*-butyl hydroperoxide (TBHP) (500 µM in PBS) was then added and the cells were incubated for additional 30 min. The fluorescence signal of DCF produced by the reaction of DCFDA reagent with ROS was then measured ( $\lambda_{\text{exc}}$  485 nm,  $\lambda_{\text{em}}$  535 nm) using a Tristar LB941 Spectrofluorimeter (Berthold Technologies, Germany). Values of treated cells were normalized to non-treated cells (100% intensity).

### 2.2.12. Antioxidant effect of quercetin on UVB irradiated NHEK cells

NHEK cells were seeded at 30,000 cells per well in a 24-well plate. They were allowed to settle for 24 h before treatment for 2 more hours with 5 µg/mL of the crude quercetin, Q-LNC POx or Q-LNC PEG preparations. Cells were then incubated with 20 µM DCFDA in a serum free medium for 30 min before a 100 mJ/cm<sup>2</sup> UVB irradiation was triggered. The cells were harvested and cellular fluorescence was assessed by flow cytometry (Canto, Becton Dickinson) directly after irradiation ([Masaki et al., 2009](#)). Data were processed using FlowJo software. Values of treated cells were normalized to non-treated cells (representing the cells with 100% ROS intensity).

### 2.2.13. Statistical analysis

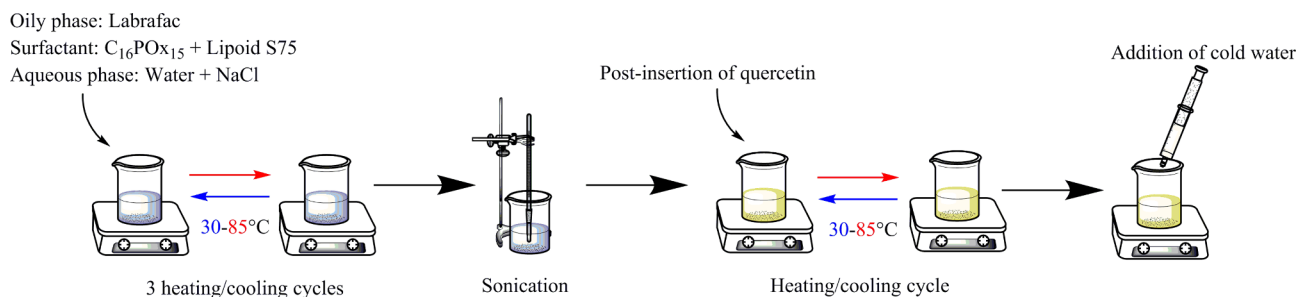
The statistical analysis of the data resulting from the cell viability and the antioxidant effect on cells was conducted with Origin Pro software 8.1 (OriginLab, USA). A one-sample *t*-test with equal variance was performed to compare cell viability and antioxidant effect with formulations to viability of untreated cells (100%). A two-sample *t*-test with unequal variance was carried out to compare cell viability of formulations two by two. The *P* value reflects the significance with \**P* < 0.05, \*\**P* < 0.01 and \*\*\**P* < 0.001.

## 3. Results and discussion

### 3.1. LNC formulation and characterization

The amphiphilic nonionic POx polymer (C<sub>16</sub>POx<sub>15</sub>) used in this study is highly soluble in water and has a molecular weight of 1520 g/mol. It possesses a low viscosity (e.g. PEtOx 50 kDa [ $\eta$ ] = 0.23 dL/g) and a high stability towards degradation ([Lorson et al., 2018](#)). Its solubility in water remains constant with temperature (no LCST characteristic for this poly(-2-methyl-2-oxazoline) POx derivative) ([Glassner et al., 2018](#)), impeding the use of the phase inversion process developed by Heurtault et al ([Heurtault et al., 2002](#)) to produce LNC. As a consequence, the protocol to form POx based LNC was redefined as represented in [Scheme 1](#). Heating and cooling cycles were first performed to solubilize and homogenize the system by melting and mixing the solid lipids (Lipoid® S75) with the liquid lipids (Labrafac®). Then, a short sonication step supplied the energy necessary to disperse the preparation ([Cohen et al., 2013](#)) and reduce its size from 300 nm to 30 nm. Quercetin was added to the mixture to produce antioxidant LNC after this stage, thus avoiding its degradation from ultrasonic energy ([Qiao et al., 2014](#)). One of the advantages of this process is thus to preserve active compound (AC) sensitive to many temperature cycles and ultrasound treatments by post-insertion into the LNC. One last heating and cooling cycle was performed to favor quercetin loading. Then, the mixture was heated at 85 °C and cold water (4 °C) was rapidly introduced to anchor the system and generate LNC stabilized by poly-oxazoline (LNC POx).

Using this process, a pre-formulation work was conducted to determine the suitable composition leading to the most stable nanosized LNC, with the lowest amount of POx and resulting in the highest drug loading. The POx concentration range explored varied from 10 to 20 mass percent, the Labrafac® oily phase from 10 to 25 mass percent and water from 55 to 80 mass percent, whereas the phospholipids Lipoid® S75 and NaCl were respectively fixed at 1.5 mass percent and 3 mass percent. The stability was evaluated from DLS measurement (data not



Scheme 1. Process of lipid nanocapsules formulation.

**Table 2**  
Characteristics of LNC POx.

	B-LNC POx	Q-LNC POx
Hydrodynamic diameter (nm)	30.5 ± 1.5	26.4 ± 0.6
PDI	0.16 ± 0.01	0.18 ± 0.01
Hydrodynamic diameter after centrifugation (nm)	30.0 ± 3	27.0 ± 2
PDI after centrifugation	0.20 ± 0.03	0.19 ± 0.01
Hydrodynamic diameter after freezing (nm)	33.6	25.8
PDI after freezing	0.16	0.17
Zeta potentiel (mV)	5.1 ± 18.4	7.9 ± 12.5
Drug loading (%)		7.9 ± 0.1
Encapsulation efficiency (%)		93 ± 1

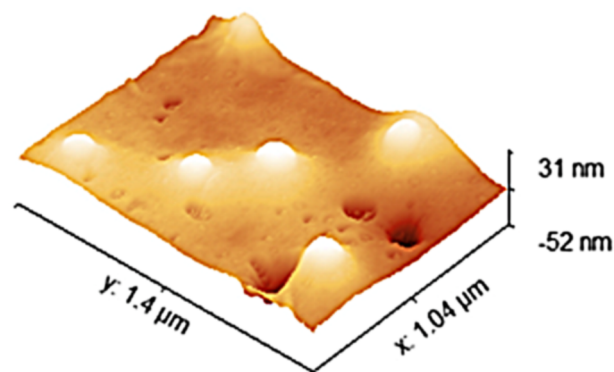


Fig. 1. LNC POx topography from AFM measurement.

shown).

As a result, POx was introduced at 20 mass percent, Labrafac® oil at 15 mass percent and water 65 mass percent. Other components such as NaCl and Lipoid® S75 were added at 3 mass percent and 1.5 mass percent. The physicochemical and morphological properties of blank LNC (B-LNC POx) and LNC loaded with quercetin (Q-LNC POx) were fully characterized; their main properties are gathered in Table 2. The hydrodynamic diameter of B-LNC was measured by DLS at  $30.5 \pm 1.5$  nm with a polydispersity index (PDI) of 0.16. Loading with quercetin (Q-LNC POx) resulted in almost similar hydrodynamic diameter ( $26.4 \pm 0.6$  nm with a PDI of  $0.18 \pm 0.01$ , Table 2). The zeta potential for both LNC was close to neutral, indicating that POx chains at the surface of the LNC stabilize the formulation by steric repulsions. LNC PEG, free and loaded with quercetin were prepared using Hatahet et al. protocol (Hatahet et al., 2017) for comparative purposes. The hydrodynamic diameter of B-LNC PEG and Q-LNC PEG were measured at 34.7 nm and 33.5 nm with a PDI of 0.03 and 0.05, respectively. As for LNC POx, the presence of quercetin did not change the LNC size.

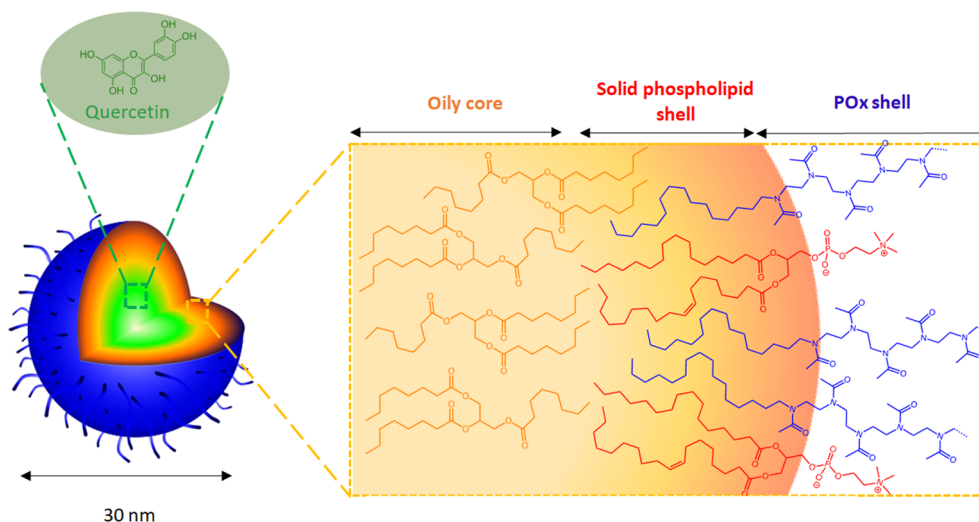
The morphology of LNC was observed by TEM after coloration with uranyl acetate solution. Well-defined spherical particles of similar size ( $< 70$  nm) were observed for both B-LNC POx and Q-LNC POx. A typical image obtained with Q-LNC POx is presented on Fig. S1. The spherical shape was confirmed by AFM (Fig. 1). It also allowed determination of the nanoparticle stiffness using the tapping mode to evaluate the contact force and more especially the repulsive force of the nanoparticle by decreasing the amplitude (setpoint). The topography of the LNC POx showed a positive phase indicating a repulsive force and mechanical properties. The latter were quantified using the harmoniX mode for determination of the indentation modulus (DMT). The DMT profile of Q-LNC POx was measured at 1–2 GPa (Fig. S2) and the associated topography profiles resulted in no permanent morphology deformation (Figs. S3 and S4) up to a constraint of about 10–20 nN. This evidences the mechanical properties of the LNC POx composed of a rigid capsule embedding on oily core just like the ones designed by Heurtault et al. (2002) for which a contact force  $> 10$  nN was applied.

It is reasonable to assume that the stiffness of the POx-based

nanoparticles results from the rigid capsule made of phospholipids from the Lipoid® S75 and POx surrounding the oily core of Labrafac® as for the LNC produced with polyethylene glycol (15)-hydroxystearate as a surfactant (Heurtault et al., 2002). For LNC POx, the amphiphilic non ionic POx stabilized the hydrophobic part of the formulation into spherical nano-objects covered with the POx chains as previously described for similar amphiphilic POx Korchia et al., 2015). An illustrative representation of the assembly is depicted in Scheme 2.

LNC formulations are well known for their high stability to dilution, centrifugation and over the long term (Huynh et al., 2009). These properties were also investigated for the newly developed POx based LNC. The LNC POx stability to dilution by 1000 (data not shown) and to high speed centrifugation at 15 000 rpm for 15 min at 25 °C was evaluated. The size and the PDI remained the same as reported in Table 2. Interestingly, after 5 days at  $-22$  °C the LNC POx hydrodynamic diameter did not change. The long term stability of B-LNC POx was assessed at 4, 25 and 37 °C by measuring the hydrodynamic diameter and PDI over a period of one month (Fig. 2). At each temperature, the size of the particles slightly increased in the first 7 days (from 30 to 38 nm at 4 °C, 42 nm at 25 °C and 49 nm at 37 °C), after 7 days the PDI remained almost identical at a low value of  $\sim 0.1$ , indicating stable monodisperse preparations. In any case, after a month, the size of the B-LNC POx remained well below 100 nm, which is fully compatible for topical delivery applications. It is noteworthy to mention that after 2 months at 25 °C, the size of the B-LNC POx had only marginally increased; it reached 57 nm whereas it was 52 nm one month before ( $PDI < 0.1$ ).

A cell viability test was first conducted on mice fibroblasts (NIH3T3) to ensure that the platform was non toxic by itself. B-LNC POx and B-LNC PEG were both tested from 1 to 50 µg/mL to evaluate the IC<sub>50</sub> (cell viability) (Fig. S5). The IC<sub>50</sub> (cell viability) value was  $43 \pm 8$  µg/mL for B-LNC PEG and  $45 \pm 8$  µg/mL for B-LNC POx and the statistical analysis did not reveal any difference in term of cell viability. Thus, the cell viability in presence of B-LNC POx seems to be well-suited for topical delivery of AC as it is similar to that of B-LNC PEG.



Scheme 2. Inner assembly of LNC POx.

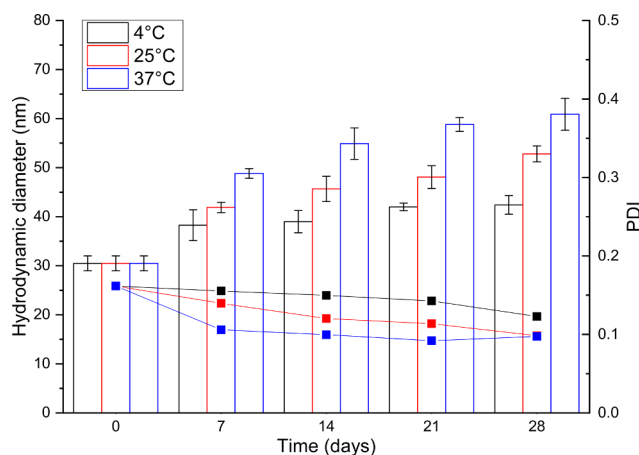


Fig. 2. Hydrodynamic diameter (column) and PDI (symbol) of B-LNC POx at 4, 25 and 37 °C over time (n = 3).

### 3.2. Quercetin loaded LNC and scavenging capacity

The LNC POx was then loaded with an AC model to evaluate the encapsulation capacity and protection of bioactivity. The natural antioxidant quercetin was chosen for its hydrophobic nature, poor solubility and sensitivity to oxidation. The post-insertion method successfully led to a high encapsulation efficiency (EE) of  $93 \pm 1\%$  corresponding to a drug loading (DL) of  $7.9 \pm 0.1\%$ . Addition of ethanol (from 100  $\mu$ L to 500  $\mu$ L) had no impact on DL and rather tended to destabilize the LNC by creating two phases, contrary to Q-LNC PEG synthesized by Hatahet et al. adapted from Heurtault protocol (Hatahet et al., 2017). Compared to others LNC (Barras et al., 2009) and NLC (Chen-yu et al., 2012; Pivetta et al., 2019) developed to encapsulate quercetin, it has to be mentioned that Q-LNC POx exhibits the highest drug loading, which exceed that obtained with Q-LNC PEG (Hatahet et al., 2017) using Cremophor and ethanol to reach a drug loading of  $2.6 \pm 0.1\%$  with an encapsulation efficiency of  $96.4 \pm 1.2\%$ . Moreover, Q-LNC POx preparation also improved quercetin loading compared to the POx stabilized mixed-micelles we recently developed (Simon et al., 2019) (from 3.6 to 7.9%).

The stability of Q-LNC POx with time was investigated at 4 °C, a temperature relevant in the presence of quercetin that is sensitive to thermal degradation (Wang and Zhao, 2016). As for the blank LNC POx, the size of quercetin loaded nanocapsules slightly evolved over one month, from 26 nm to 40 nm with a PDI staying under 0.2 (Fig. 3). As

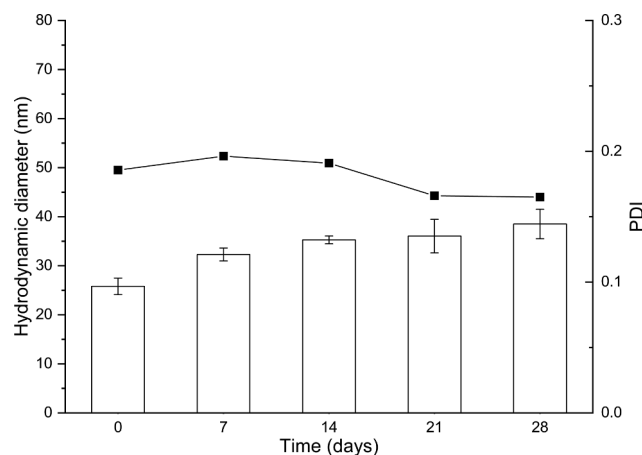


Fig. 3. Hydrodynamic diameter (column) and PDI (symbol) of Q-LNC POx at 4 °C with time (n = 3).

for B-LNC POx, Q-LNC POx was also stable to dilution and centrifugation (Table 2).

The stability study of Q-LNC POx was completed by evaluating the quercetin leakage from the nanocapsules in aqueous media (Fig. S6). After 7 h, only 1.5% of quercetin was released from Q-LNC POx and it reached a low value of 5% after 48 h. This result confirmed that quercetin is localized within the core of the LNC. Interestingly, the LNC POx formulation reduced by four times the quercetin leakage in aqueous media compared to the mixed-micelles formulation (Simon et al., 2019). The Q-LNC POx also seemed to better retain quercetin than Q-LNC PEG that showed a leakage of quercetin of almost 15% after 24 h using the same experimental conditions (Hatahet et al., 2017). This result might be due to the rigid capsule surrounding the oily core acting as a sealed reservoir and ensuring a high stability for the particles.

Antioxidant tests were performed in order to evaluate the ability of the LNC POx platform to protect and maintain the bioactivity of the encapsulated compound. The radical scavenging capacity was assessed *in vitro* using a chemical assay (DPPH). It was also evaluated on mice fibroblasts and human keratinocytes by generating reactive oxygen species (ROS) respectively using organic peroxide and UVB irradiation.

The quercetin antioxidant is able to react with the 2,2-diphenyl-1-picrylhydrazyl (DPPH<sup>•</sup>) molecule by its free radical on the hydrazine position leading to DPPHH. The radical scavenging capacity of quercetin encapsulated in the Q-LNC POx was assessed by looking at its inhibitive interaction with DPPH<sup>•</sup>. The IC<sub>50</sub> (DPPH<sup>•</sup> inhibition) value

deduced from the DPPH<sup>•</sup> decrease shows higher antioxidant activity for Q-LNC POx ( $IC_{50}$  (DPPH<sup>•</sup> inhibition) = 2  $\mu$ g/mL) than for crude quercetin, which exhibited a twice higher  $IC_{50}$  (Fig. S7). The higher antioxidant activity of Q-LNC POx can be due to a better protection of the antioxidant to oxidation, a greater conformation or organization in the nanocapsule compared to crude quercetin.

### 3.3. Quercetin loaded antioxidant activity

To go further in the evaluation of the antioxidant effect of Q-LNC POx with respect to classical PEG based LNC, both POx and PEG based Q-LNC were loaded at the same quercetin concentration and tested on mice fibroblasts and human keratinocytes. A cell viability test was performed on NIH3T3 to determine the maximum non toxic quercetin concentration to be used for the antioxidant tests. The  $IC_{50}$  (cell viability) values were determined for crude quercetin (17.5  $\mu$ g/mL), Q-LNC POx (23  $\mu$ g/mL) and Q-LNC PEG (16  $\mu$ g/mL) (Fig. S8). The cell viability of blank LNCs was also evaluated B-LNC POx (43  $\mu$ g/mL) and B-LNC PEG (45  $\mu$ g/mL).

As for the uncharged POx and PEG-based LNC, the  $IC_{50}$  (cell viability) value is not affected by the nature of the stabilizing polymer.

To perform the antioxidant study, the concentration of quercetin was selected such as to avoid formulation toxicity from the cell viability results; it was set at 5  $\mu$ g/mL. The radical scavenging capacity of Q-LNC POx was first tested on NIH3T3 and compared to Q-LNC PEG and crude quercetin (Fig. 4). Cells were treated with the formulations for 24 h, then an oxidative stress was induced by *tert*-butyl hydroperoxide (TBHP). The quantity of ROS generated was determined by fluorescence spectroscopy using the DCFDA probe. The results were normalized to untreated cells with TBHP exposure (non treated). The crude quercetin was able to reduce excess ROS generation to  $69 \pm 6\%$  ( $P < 0.01$ ) and similarly Q-LNC POx decreased surplus ROS to  $70 \pm 6\%$  ( $P < 0.01$ ). Q-LNC PEG was less able to counter ROS generation with a reduction to  $81 \pm 9\%$  ( $P < 0.01$ ). The antioxidant activity of quercetin once loaded in LNC POx was thus maintained and even slightly enhanced compared to Q-LNC PEG. B-LNC POx was also tested and the cells resisted to the peroxides generated reflecting the innocuousness of POx upon oxidation.

Another antioxidant test was performed on human keratinocytes with UV irradiation as a source of ROS. Therefore, the antioxidant effect observed on mice fibroblasts can be transposed to human cells with ROS simulated from an environmental factor.

We first evaluated the scavenging activity of ROS naturally generated by the cells (Table 3, “No UV irradiation”). The fluorescence

**Table 3**

ROS relative intensity for crude quercetin, Q-LNC POx and Q-LNC PEG at a quercetin concentration of 5  $\mu$ g/mL ( $n = 3$ ) on human keratinocytes. Fluorescence intensity was normalized to irradiated cells (not treated with formulation). A one sample *t*-test relative to untreated cells was performed (\*:  $P < 0.05$ , \*\*:  $P < 0.01$  and \*\*\*:  $P < 0.001$ ).

Conditions	No UV irradiation	UV irradiation
	ROS relative intensity (%)	ROS relative intensity (%)
Untreated	100	100
Crude quercetin	$59 \pm 19$ **	$65 \pm 6$ **
Q-LNC POx	$91 \pm 16$	$83 \pm 4$ **
Q-LNC PEG	$94 \pm 13$	$91 \pm 15$

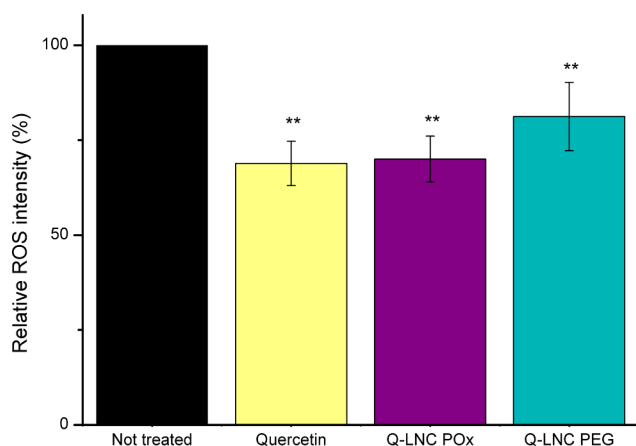
intensity was normalized to untreated cells (no formulation and no UV irradiation). UV irradiation was then carried out to evaluate the antioxidant capacity on overproduction of ROS (Table 3, “UV irradiation” column). The results were normalized to untreated cells. As shown in Table 3, the crude quercetin significantly reduced the ROS naturally produced by the cells to  $59 \pm 19\%$  ( $P < 0.01$ ) which is not the case for Q-LNC POx and Q-LNC PEG maintaining a quantity of ROS of  $91 \pm 16\%$  and  $94 \pm 13\%$  respectively. On the contrary, once the cells irradiated, the crude quercetin was the one reducing most of the ROS over generated to  $65 \pm 6\%$  ( $P < 0.01$ ) whereas Q-LNC POx was able to reduce ROS at  $83 \pm 4\%$  ( $P < 0.01$ ) and Q-LNC PEG at  $91 \pm 15\%$ . The statistical analysis revealed that crude quercetin and Q-LNC POx significantly decreased the ROS over generated. Therefore, Q-LNC POx was able to maintain the antioxidant activity of quercetin alike Q-LNC PEG. It has to be noticed that, even if the crude quercetin reduced most of the ROS, its too powerful activity could scavenge the ROS essential for cell survival.

### 4. Conclusion

This work demonstrates the ability of amphiphilic non ionic polyoxazolines (POx) to act as a surfactant to form lipid based nanoformulation suitable for topical delivery of quercetin. The optimized nanoformulation allows to shape well-defined monodisperse spherical lipid nanocapsules (LNC) of 30 nm diameter size. They are composed of a Labrafac<sup>®</sup> oily core stabilized by a solid phospholipid and POx surfactant shell, whose stiffness ensured a high stability over time, centrifugation, freezing and dilution. Most importantly, LNC POx are free from the PEG-dependant inversion process universally used to date to design LNC. The process developed here associates a sonication step to heating/cooling cycles allowing loading the natural antioxidant quercetin at a high drug loading of  $7.9 \pm 0.1\%$  without inducing any morphological change in the particles nor altering their stability. Interestingly, the LNC POx leads to a higher encapsulation and a slightly better radical scavenging capacity on mice fibroblasts and human keratinocytes than LNC PEG. This evidences the crucial role amphiphilic polyoxazolines might take in the future as PEG free topical delivery platform for topical and intravenous administration for applications in nanomedicine, dermatology and cosmetics.

### CRediT authorship contribution statement

**L. Simon:** Conceptualization, Formal analysis, Methodology, Validation, Investigation, Writing - original draft, Writing - review & editing, Visualization. **V. Lapinte:** Conceptualization, Methodology, Writing - review & editing, Visualization, Supervision, Project administration. **L. Lionnard:** Methodology, Investigation, Writing - original draft, Writing - review & editing. **N. Marcotte:** Conceptualization, Methodology, Writing - review & editing, Visualization, Supervision, Project administration. **M. Morille:** Methodology, Writing - review & editing, Resources, Supervision. **A. Aouacheria:** Methodology,



**Fig. 4.** ROS relative intensity for crude quercetin, Q-LNC POx and Q-LNC PEG at a quercetin concentration of 5  $\mu$ g/mL ( $n = 3$ ) on NIH3T3 cells. Fluorescence intensity was normalized to TBHP treated cells without formulation. A one sample *t*-test relative to untreated cells was performed (\*:  $P < 0.05$ , \*\*:  $P < 0.01$  and \*\*\*:  $P < 0.001$ ).

Resources, Writing - review & editing. **K. Kissa:** Resources. **J.M. Devoisselle:** Resources, Project administration. **S. Bégu:** Conceptualization, Methodology, Writing - review & editing, Visualization, Supervision, Project administration.

## Declaration of Competing Interest

The authors declare that they have no known competing financial interests or personal relationships that could have appeared to influence the work reported in this paper.

## Acknowledgements

The authors thank Michel Ramonda (CTM, Univ Montpellier, France) for help on AFM measurements, Christophe Dorandeu (ICGM, Univ Montpellier, France) for assistance on HPLC analysis and Thomas Cacciaguerra (ICGM, Univ Montpellier, France) for assistance on TEM experiments. We acknowledge the imaging facility MRI, member of the national infrastructure France-BioImaging infrastructure supported by the French National Research Agency (ANR-10-INBS-04, «Investments for the future») for Cytometry Analysis.

## Appendix A. Supplementary material

Supplementary data to this article can be found online at <https://doi.org/10.1016/j.ijpharm.2020.119126>.

## References

- Abdel-Mottaleb, M.M.A., Neumann, D., Lamprecht, A., 2011. Lipid nanocapsules for dermal application: a comparative study of lipid-based versus polymer-based nanocarriers. *Eur. J. Pharm. Biopharm.* 79, 36–42.
- Anton, N., Gayet, P., Benoit, J.-P., Saulnier, P., 2007. Nano-emulsions and nanocapsules by the PIT method: an investigation on the role of the temperature cycling on the emulsion phase inversion. *Int. J. Pharm.* 344, 44–52.
- Barras, A., Mezzetti, A., Richard, A., Lazzaroni, S., Roux, S., Melnyk, P., Betbeder, D., Monfiliette-Dupont, N., 2009. Formulation and characterization of polyphenol-loaded lipid nanocapsules. *Int. J. Pharm.* 379, 270–277.
- Blois, M.S., 1958. Antioxidant determinations by the use of a stable free radical. *Nature* 181, 1199–1200.
- Chen-yu, G., Chun-fen, Y., Qi-lu, L., Qi, T., Yan-wei, X., Wei-na, L., Guang-xi, Z., 2012. Development of a Quercetin-loaded nanostructured lipid carrier formulation for topical delivery. *Int. J. Pharm.* 430, 292–298.
- Cohen, J., Deloid, G., Pyrgiotakis, G., Demokritou, P., 2013. Interactions of engineered nanomaterials in physiological media and implications for in vitro dosimetry. *Nanotoxicology* 7, 417–431.
- Dargaville, T.R., Park, J.-R., Hoogenboom, R., 2018. Poly(2-oxazoline) hydrogels: state-of-the-art and emerging applications. *Macromol. Biosci.* 18, 1800070.
- Dragicevic, N., Atkinson, J.P., Maibach, H.I., 2015. Chemical penetration enhancers: classification and mode of action. In: Dragicevic, N., Maibach, H.I. (Eds.), *Percutaneous Penetration Enhancers Chemical Methods in Penetration Enhancement: Modification of the Stratum Corneum*. Springer, Berlin Heidelberg, Berlin, Heidelberg, pp. 11–27.
- Elias, P.M., 1983. Epidermal lipids, barrier function, and desquamation. *J. Invest. Dermatol.* 80, S44–S49.
- Garcês, A., Amaral, M.H., Sousa Lobo, J.M., Silva, A.C., 2018. Formulations based on solid lipid nanoparticles (SLN) and nanostructured lipid carriers (NLC) for cutaneous use: a review. *Eur. J. Pharm. Sci.* 112, 159–167.
- Glassner, M., Vergaen, M., Hoogenboom, R., 2018. Poly(2-oxazoline)s: a comprehensive overview of polymer structures and their physical properties. *Polym. Int.* 67, 32–45.
- Guillerm, B., Monge, S., Lapinte, V., Robin, J.-J., 2012. How to modulate the chemical structure of polyoxazolines by appropriate functionalization. *Macromol. Rapid Commun.* 33, 1600–1612.
- Hatahet, T., Morille, M., Hommoss, A., Devoisselle, J.M., Müller, R.H., Bégu, S., 2016. Quercetin topical application, from conventional dosage forms to nanodosage forms. *Eur. J. Pharm. Biopharm.* 108, 41–53.
- Hatahet, T., Morille, M., Hommoss, A., Devoisselle, J.M., Müller, R.H., Bégu, S., 2018. Liposomes, lipid nanocapsules and smartCrystals®: a comparative study for an effective quercetin delivery to the skin. *Int. J. Pharm.* 542, 176–185.
- Hatahet, T., Morille, M., Shamseddin, A., Aubert-Pouessel, A., Devoisselle, J.M., Bégu, S., 2017. Dermal quercetin lipid nanocapsules: Influence of the formulation on antioxidant activity and cellular protection against hydrogen peroxide. *Int. J. Pharm.* 518, 167–176.
- Heurtault, B., Saulnier, P., Pech, B., Proust, J., Benoit, J.-P., 2002. A Novel Phase Inversion-Based Process for the Preparation of Lipid Nanocarriers.
- Huynh, N.T., Passirani, C., Saulnier, P., Benoit, J.P., 2009. Lipid nanocapsules: a new platform for nanomedicine. *Int. J. Pharm.* 379, 201–209.
- Korchia, et al., 2015. Photodimerization as an alternative to photocrosslinking of nanoparticles: proof of concept with amphiphilic linear polyoxazoline bearing coumarin unit. *Polym. Chem.* 6 (33), 6029–6039. <https://doi.org/10.1039/C5PY00834D>.
- Krutmann, J., Bouloc, A., Sore, G., Bernard, B.A., Passeron, T., 2017. The skin aging exposome. *J. Dermatol. Sci.* 85, 152–161.
- Lorson, T., Lübtow, M.M., Wegener, E., Haider, M.S., Borova, S., Nahm, D., Jordan, R., Sokolski-Papkov, M., Kabanov, A.V., Luxenhofer, R., 2018. Poly(2-oxazoline)s based biomaterials: a comprehensive and critical update. *Biomaterials* 178, 204–280.
- Lubich, C., Allacher, P., de la Rosa, M., Bauer, A., Prenninger, T., Horling, F.M., Siekmann, J., Oldenburg, J., Scheiflinger, F., Reipert, B.M., 2016. The mystery of antibodies against polyethylene glycol (PEG) - what do we know? *Pharm. Res.* 33, 2239–2249.
- Maherani, et al., 2011. Liposomes: A Review of Manufacturing Techniques and Targeting Strategies. *Current Nanosci.* 7 (3), 436–452.
- Masaki, H., Izutsu, Y., Yahagi, S., Okano, Y., 2009. Reactive oxygen species in HaCaT keratinocytes after UVB irradiation are triggered by intracellular Ca<sup>2+</sup> levels. *J. Invest. Dermatol. Symp. Proc.* 14, 50–52.
- Montenegro, et al., 2016. From nanoemulsions to nanostructured lipid carriers: a relevant development in dermal delivery of drugs and cosmetics. *J. Drug Delivery Sci. Technol.* 32, 100–112.
- Moreadith, R.W., Viegas, T.X., Bentley, M.D., Harris, J.M., Fang, Z., Yoon, K., Dizman, B., Weimer, R., Rae, B.P., Li, X., Rader, C., Standaert, D., Olanow, W., 2017. Clinical development of a poly(2-oxazoline) (POZ) polymer therapeutic for the treatment of Parkinson's disease – proof of concept of POZ as a versatile polymer platform for drug development in multiple therapeutic indications. *Eur. Polym. J.* 88, 524–552.
- Nagula, R.L., Wairkar, S., 2019. Recent advances in topical delivery of flavonoids: a review. *J. Control. Release* 296, 190–201.
- Pivetta, T.P., Silva, L.B., Kawakami, C.M., Araújo, M.M., Del Lama, M.P.F.M., Naal, R.M.Z.G., Maria-Engler, S.S., Gaspar, L.R., Marcato, P.D., 2019. Topical formulation of quercetin encapsulated in natural lipid nanocarriers: evaluation of biological properties and phototoxic effect. *J. Drug Delivery Sci. Technol.* 53, 101148.
- Qiao, L., Sun, Y., Chen, R., Fu, Y., Zhang, W., Li, X., Chen, J., Shen, Y., Ye, X., 2014. Sonochemical effects on 14 flavonoids common in citrus: relation to stability. *PLoS ONE* 9, e87766.
- Roberts, M.S., Mohammed, Y., Pastore, M.N., Namjoshi, S., Yousef, S., Alinaghi, A., Haridass, I.N., Abd, E., Leite-Silva, V.R., Benson, H.A.E., Grice, J.E., 2017. Topical and cutaneous delivery using nanosystems. *J. Control. Release* 247, 86–105.
- Rudmann, D.G., Alston, J.T., Hanson, J.C., Heidel, S., 2013. High molecular weight polyethylene glycol cellular distribution and PEG-associated cytoplasmic vacuolation is molecular weight dependent and does not require conjugation to proteins. *Toxicol. Pathol.* 41, 970–983.
- Sala, M., Diab, R., Elaissari, A., Fessi, H., 2018. Lipid nanocarriers as skin drug delivery systems: properties, mechanisms of skin interactions and medical applications. *Int. J. Pharm.* 535, 1–17.
- Schäfer-Korting, M., Mehnert, W., Korting, H.-C., 2007. Lipid nanoparticles for improved topical application of drugs for skin diseases. *Adv. Drug Deliv. Rev.* 59, 427–443.
- Simon, L., Vincent, M., Le Saux, S., Lapinte, V., Marcotte, N., Morille, M., Dorandeu, C., Devoisselle, J.M., Bégu, S., 2019. Polyoxazolines based mixed micelles as PEG free formulations for an effective quercetin antioxidant topical delivery. *Int. J. Pharm.* 118516.
- Viegas, T.X., Fang, Z., Yoon, K., Weimer, R., Dizman, B., 2018. 6-Poly(oxazolines). In: Parambath, A. (Ed.), *Engineering of Biomaterials for Drug Delivery Systems*. Woodhead Publishing, pp. 173–198.
- Wang, J., Zhao, X.H., 2016. Degradation kinetics of fisetin and quercetin in solutions affected by medium pH, temperature and co-existing proteins. *J. Serb. Chem. Soc.* 81, 243–254.
- Yang, L., Li, P., Gao, Y.-J., Li, H.-F., Wu, D.-C., Li, R.-X., 2009. Time Resolved UV-Vis Absorption Spectra of Quercetin Reacting with Various Concentrations of Sodium Hydroxide.
- Zalipsky, S., Hansen, C.B., Oaks, J.M., Allen, T.M., 1996. Evaluation of blood clearance rates and biodistribution of poly(2-oxazoline)-grafted liposomes. *J. Pharm. Sci.* 85, 133–137.
- Zhai, Y., Yang, X., Zhao, L., Wang, Z., Zhai, G., 2014. Lipid nanocapsules for transdermal delivery of ropivacaine: in vitro and in vivo evaluation. *Int. J. Pharm.* 471, 103–111.
- Zhai, Zhai, 2014. Advances in lipid-based colloid systems as drug carrier for topic delivery. *J. Controlled Release* 193, 90–99.
- Zhang, P., Sun, F., Liu, S., Jiang, S., 2016. Anti-PEG antibodies in the clinic: Current issues and beyond PEGylation. *J. Control. Release* 244, 184–193.